ACCOUNTS
of chemical research

Conformational Analyses of the Reaction Coordinate of Glycosidases

GIDEON J. DAVIES,*,† ANTONI PLANAS,‡ AND CARME ROVIRA*,§,∥

†*Structural Biology Laboratory, Department of Chemistry, The University of York, YO10 5DD, United Kingdom,* ‡*Laboratory of Biochemistry, Institut Químic de Sarrià, Universitat Ramon Llull, c/Via Augusta 390, 08017 Barcelona, Spain,* §*Computer Simulation & Modeling and Institut de Química Teòrica i Computacional (IQTCUB), Parc Científic de Barcelona, Baldiri Reixac 4, 08028 Barcelona, Spain, and* ∥*Institució Catalana de Recerca i Estudis Avançats (ICREA), Passeig Lluís Companys 23, 08018 Barcelona, Spain*

RECEIVED ON JULY 1, 2011

CONSPECTUS

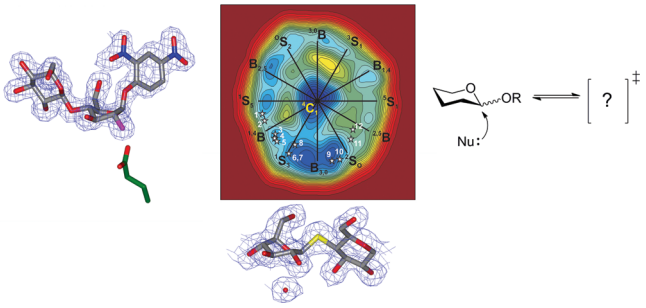

The enzymatic hydrolysis of the glycosidic bond is catalyzed by diverse enzymes generically termed glycoside hydrolases (hereafter GHs) or glycosidases. The many sequence-based families of glycosidases have served as a rich hunting ground for enzymologists for years. Not only are these enzymes of fundamental interest, providing paradigms for enzymatic catalysis that extend beyond the bounds of carbohydrate chemistry, but the enzymes themselves play myriad essential roles in diverse biological processes. The wide utility of glycosidases, from their industrial harnessing in the hydrolysis of plant biomass to their roles in human physiology and disease, has engendered a large scientific constituency with an interest in glycosidase chemistry.

A fascinating thread of this research, and one with major impact on the design of enzyme inhibitors, is the conformational analysis of reaction pathways within the diverse families. These GH families provide a large pallet of enzymes with which chemists have attempted to depict the conformational landscape of glycosidase action. In this Account, we review three-dimensional insight into the conformational changes directed by glycosidases, primarily from structural observations of the stable enzyme–ligand species adjacent to the transition state (or states) and of enzyme–inhibitor complexes. We further show how recent computational advances dovetail with structural insight to provide a quantum mechanical basis for glycosidase action.

The glycosidase-mediated hydrolysis of the acetal or ketal bond in a glycoside may occur with either inversion or retention of the configuration of the anomeric carbon. Inversion involves a single step and transition state, whereas retention, often referred to as the double displacement, is a two-step process with two transition states. The single transition state for the inverting enzymes and the two transition states (those flanking the covalent intermediate) in the double displacement have been shown to have substantial oxocarbenium ion character. The dissociative nature of these transition states results in significant relative positive charge accumulation on the pyranose ring. The delocalization of lone-pair electrons from the ring oxygen that stabilizes the cationic transition state implies that at, or close to, the transition states the pyranose will be distorted away from its lowest energy conformation to one that favors orbital overlap.

Over the preceding decade, research has highlighted the harnessing of noncovalent interactions to aid this distortion of the sugar substrates from their lowest energy chair conformation to a variety of different boat, skew boat, and half-chair forms, each of which favors catalysis with a given enzyme and substrate. Crystallographic observation of stable species that flank the transition state (or states), of both retaining and inverting glycosidases, has allowed a description of their conformational itineraries, illustrating how enzymes facilitate the "electrophilic migration" of the anomeric center along the reaction coordinate.

The blossoming of computational approaches, such as ab initio metadynamics, has underscored the quantum mechanical basis for glycoside hydrolysis. Conformational analyses highlight not only the itineraries used by enzymes, enabling their inhibition, but are also reflected in the nonenzymatic synthesis of glycosides, wherein chemists mimic strategies found in nature.

Published on the Web 09/16/2011 www.pubs.acs.org/accounts
10.1021/ar2001765

The hydrolysis of the acetal or ketal bonds of glycosides, by the many families of glycosidases (classified into glycoside hydrolase "GH" families at www.cazy.org),[1] may occur with either retention or inversion of the configuration of the anomeric carbon, essentially as described in Koshland's insightful 1953 treatise[2] (Figure 1A,B; NAD^+ dependent "glycosidases" are not considered). There is a wealth of evidence that the single transition state (TS) for the inverting enzymes and the two transition states (those which flank the covalent intermediate) in the double displacement possess substantial oxocarbenium ion-like character. The dissociative nature of this transition state results in significant positive charge accumulation on the pyranose ring. The delocalization of lone-pair electrons from the ring oxygen that stabilizes the cationic transition state implies that at, or close to, the transition states the pyranose will be distorted away from its lowest energy conformation (for most pyranosides a chair) to one that favors such orbital overlap. Sinnott was the first to crystallize the concept that enzymes would therefore likely perform catalysis through one of two half-chair $^4H_3/^3H_4$ (or related ^4E and ^3E envelopes) or boat $^{2,5}B/B_{2,5}$ conformations[3] (Figure 1C), those that fulfill the stereochemical requirements of an oxocarbenium ion-like transition state (C5, O5, C1, and C2 atoms are almost coplanar). In this Account, we review the three-dimensional (3D) insight that has been provided into the conformational itinerary of glycosidases, primarily through structural observations of the stable enzyme–ligand species adjacent to the transition state(s) and of enzyme–inhibitor complexes. We discuss such itineraries in terms of classical puckering parameters and show how recent quantum chemical analyses of free sugars and enzymatic reaction coordinates provide an interpretative framework.

Historical Perspectives

Pyranoside ring description, following IUPAC guidelines,[4] is based upon a capital letter defining the ring shape (chair *C*, half-chair H, skew-boat S, boat B, and envelope E) with two super/subscripted numerals designating the atom(s) that lie outside of a four-atom reference plane. The description of pyranoside ring conformations, and thus the itinerary of their interconversions, is most frequently based upon the Cremer–Pople puckering parameters Q, θ, and ϕ, which

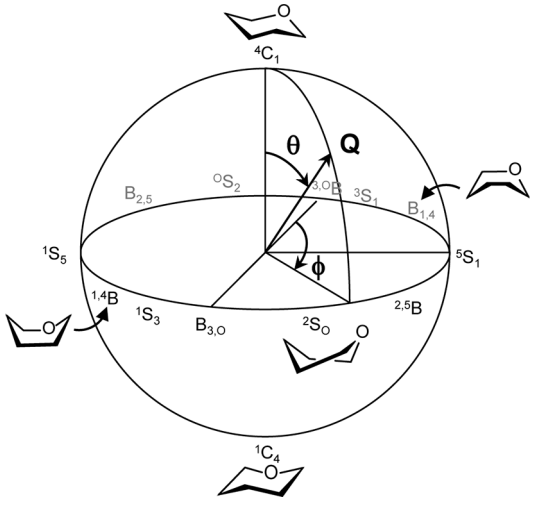

FIGURE 2. Cremer and Pople puckering coordinates of a six-membered ring (Q, θ, and ϕ) and their projection in the x,y plane (q_x and q_y).

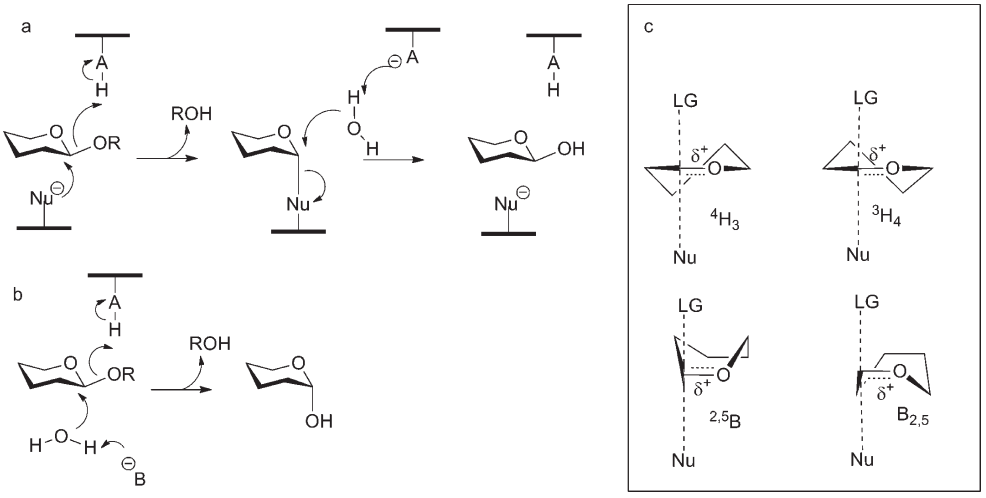

FIGURE 1. (a) Mechanism of hydrolysis of the acetal or ketal bonds of glycosides by glycosidases; shown here for attack on a β-D-glycoside with (a) net retention or (b) inversion of anomeric configuration. Inset: (c) Possible conformations of the −1 sugar ring at the transition state structure: $^4H_3$, $^3H_4$, $^{2,5}B$, and $B_{2,5}$ (related ^3E and ^4E forms are omitted).

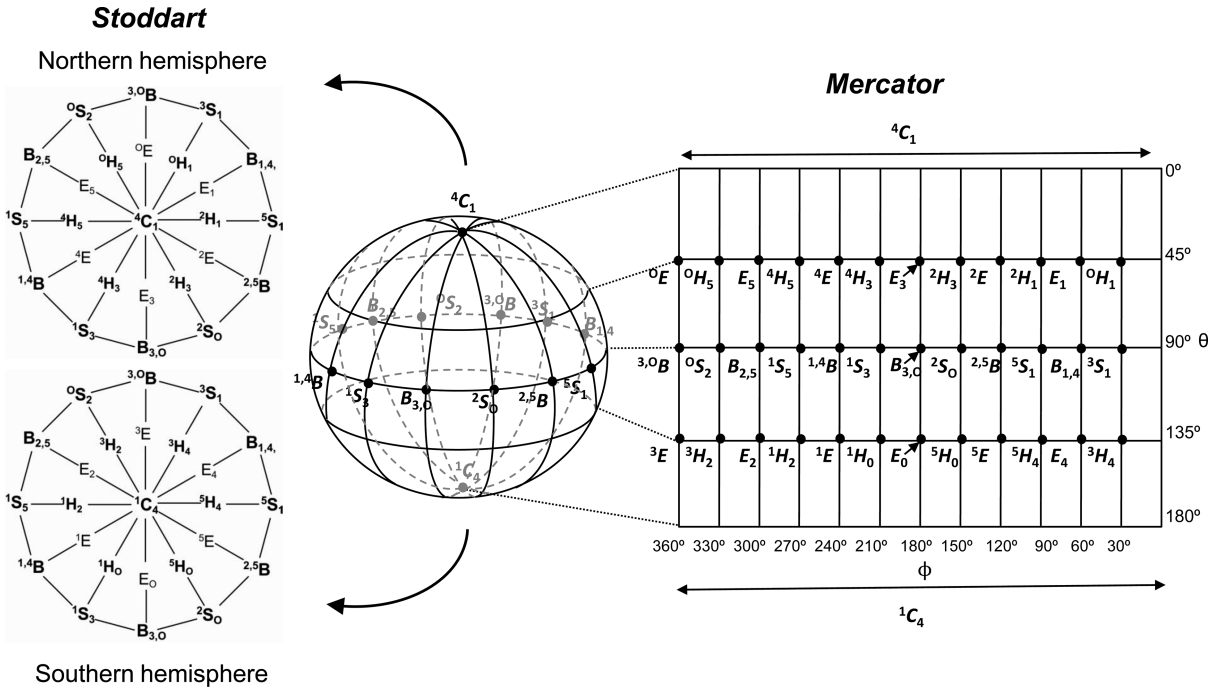

FIGURE 3. Main conformations on the Cremer–Pople sphere along with two of their most used representations: Stoddart diagram (Northern and Southern polar projections are shown) and Mercator projection.

form a "sphere" of radius Q with the classical $^4C_1$ and $^1C_4$ chairs at the North and South poles, respectively ($\theta = 0$, 180°), with the equator ($\theta = 90°$) defining a skew-boat–boat interconversion itinerary (Figure 2). For convenience, the Northern and Southern hemispheres are often projected on the pseudorotational itinerary[5] (Figure 3). Thus, the sphere itself, or more usually its "Stoddart" polar projection, provides a simple conceptual framework for defining the interconversion of different conformers during catalysis. The Mercator projection (Figure 3), analogous to global cartography, may also be used.

The seminal 3D structure determination of the first enzyme, lysozyme from hen egg white (HEWL),[6] allowed postulation of the key elements of glycosidase catalysis. Although some historical suggestions have been reconsidered,[7] proposals that glycosidases promoted formation of their transition states through distortion of the pyranoside ring of the substrate remain true. Furthermore, building upon Pauling's ideas, from the 1940s that high affinity inhibitors could be generated by mimicking the "strained activated complex",[8] "distorted" transition state mimics were shown to act as enzyme inhibitors.[9] Three-dimensional structure interpreted in light of physical organic and computational insight remains the driving force for the conformational analyses of glycosidases. In the following sections, we shall analyze distortion around each of the "Sinnott" potential TS structures and see how experiment and computation dovetail elegantly to provide detailed conformational itineraries. We do not consider complexes that "bypass" the active site or are misleading because of changes in the enzyme structure.

Pathways around the $^4H_3$ Half Chair ($^1S_3$, $^4H_3$, $^4C_1$)

$^1S_3 \leftrightarrow {}^4H_3 \leftrightarrow {}^4C_1$ Retaining β-Glycosidases. The chitobiose complex of a CAZy family GH20 chitobiase, serendipitously trapped in an unhydrolyzed form,[10] and a GH7 endoglucanase trapped with a nonhydrolyzable thio-linked oligosaccharide[11] provided the first unambiguous analyses of distorted enzyme–substrate complexes (hereafter termed "Michaelis complexes" after the E + S ↔ ES scheme of Michaelian kinetics) in 1996. The remarkable observations in both complexes were that the pyranosides in the −1 subsite (nomenclature in ref 12) were distorted to approximate ^4E and $^1S_3$ conformations, respectively, with both conformations being very close in the Stoddart diagram (Figure 3). These conformations provided a structural context both for the in-line nucleophilic attack into the σ^* antibonding orbital of the breaking C1-OR bond as well as for the reduction of steric barriers to nucleophilic attack notably by H-1 but also the 1,3 diaxial clashes to H-3 and H-5. These conformations were also consistent with potential lone-pair contribution from the endocyclic oxygen, here

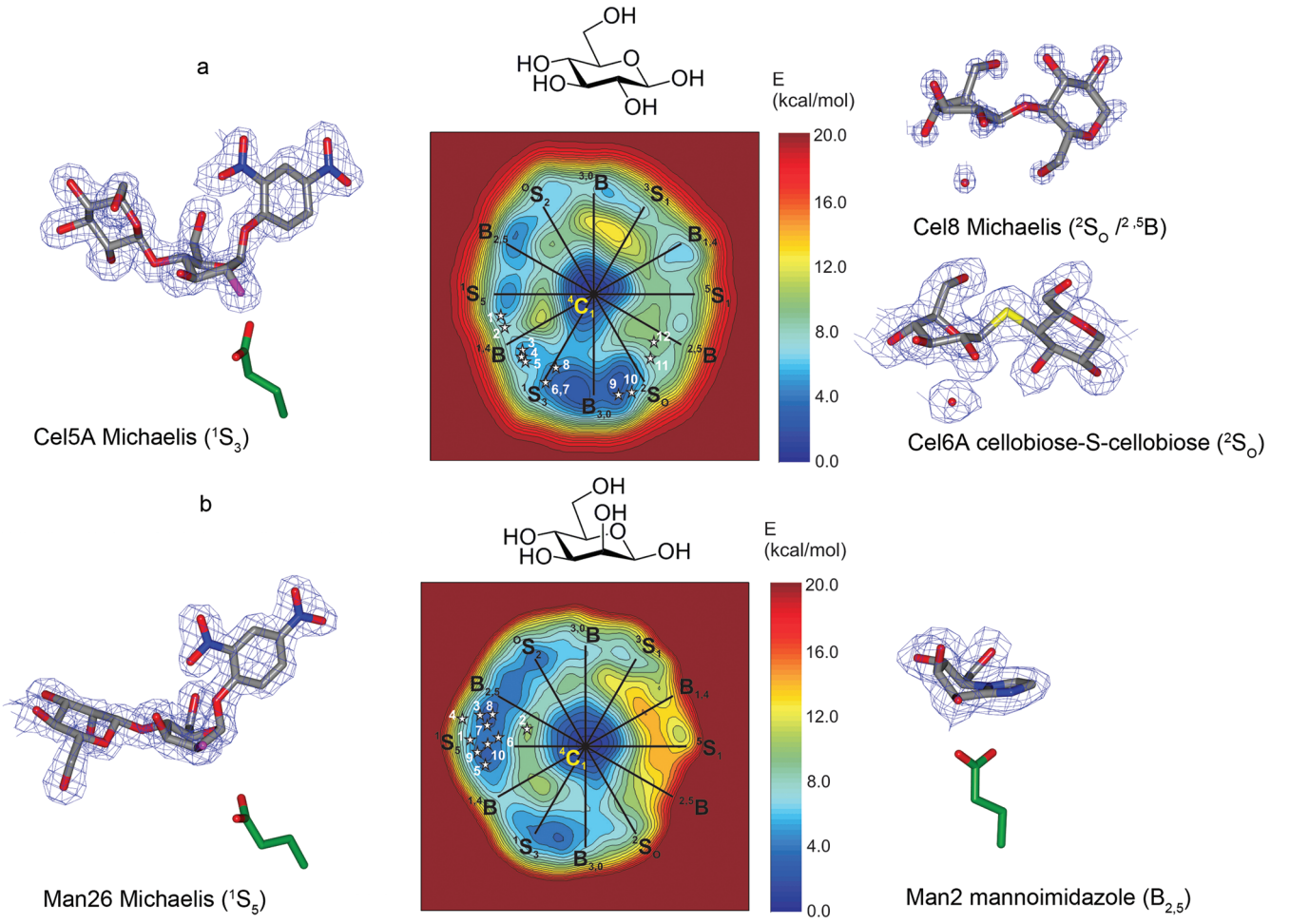

FIGURE 4. Substrate distortion in β-D-glucosidases and β-D-mannosidases. (a) *Gluco*-active enzymes: Experimental density for distorted substrate complexes of Cel5A[13] (retaining, left) and Cel6A[30] and Cel8[33] (inverting, right) trapped by different strategies (see text) along with the computed FEL of β-D-glucopyranose with respect to ring distortion. The observed conformations of β-glucosidase Michaelis complexes are represented by star symbols (PDB codes: 1eib, 1e6n, 1fcv, 1ovw, 1v03, 4a3h, 1e56, 1w2u, 1qk2, 1gz1, 1ocn, and 1kwf, from **1** to **12**, respectively). Each contour line of the diagram corresponds to 0.5 kcal·mol^{-1}. (b) *Manno*-active enzymes: Experimental electron density for the Man26A Michaelis complex[38] (left) and the mannoimidazole complex of Man2[43] (right) along with the computed FEL of β-D-mannopyranose.[23] Observed structures of β-mannosidase Michaelis and inhibitor complexes are represented by star symbols (PDB codes: 2wbk, 2vjx, 2vl4, 2vo5, 2vr4, 2vqt, 2vot, 2vmf, 1gvy, and 1gw1, from **1** to **10**, respectively).

antiperiplanar, to the departing group. Subsequently, all of the stable species along the reaction coordinate of a retaining endoglucanase, Cel5A, were trapped, providing a series of "snapshots" of the reaction pathway.[13] Again, the ES complex was observed in $^{1}S_{3}$ conformation (Figure 4a), and this species reacted to form the covalent intermediate observed in $^{4}C_{1}$ chair.

The observations described above, interpreted in light of the Stoddart diagram, suggest a "longitudinal" $^{1}S_{3} \rightarrow [^{4}H_{3}]^{\ddagger} \rightarrow {}^{4}C_{1}$ itinerary for the formation of the covalent glycosyl–enzyme intermediate by these retaining β-glycosidases consistent with an electrophilic migration of the anomeric carbon during catalysis. Thus, in the case of Cel5A, the $^{1}S_{3}$ and $^{4}C_{1}$ conformations flank the $^{4}H_{3}$ conformation through which the reaction is expected to pass at, or close to, the transition state. Subsequently, there have been many studies finding distorted sugar conformations around the $^{1,4}B/{}^{1}S_{3}/{}^{4}H_{3}/{}^{4}C_{1}$ region of the itinerary, including family GH18 chitinases,[14] GH26 β-1,4,1,3 glucanases,[15] GH39 β-xylosidases,[16] GH84 *O*-GlcNAcases,[17] as well as in modeling studies.[18] For retaining β-D-glycosidases, this is the most prevalent reaction coordinate.

A promising and complementary approach that can be used to quantify the conformational flexibility of the substrate in glycosidases is metadynamics. The method[19] is aimed at enhancing the sampling of phase space in a molecular dynamics simulation and reconstructing the free energy landscape of complex systems with respect to a

reduced number of collective variables (CVs). In carbohydrates, the use of the Cremer and Pople puckering coordinates[20] as CVs allows computation of the free energy landscape (FEL) associated to the puckering sphere or Stoddard diagram.[21,22] Provided a quantum mechanical methodology is used to compute the energy, electronic changes with ring distortion can be analyzed.[22]

Recently, it has been shown that the FEL of an isolated pyranose ring (Figure 4a) can be used to predict the conformation of the substrate in Michaelis complexes of glycosidases, as well as possible catalytic itineraries.[23] In particular, the regions connecting the lowest energy distorted conformations (Figure 4) are favored itineraries. These conformations show the best compromise among energy, structure (elongation/shortening of the C1−O1/C1−O5 bonds and "axiality" of the C1−O1 bond), and charge development at the anomeric carbon (an index integrating all these parameters was introduced in ref 23). The conformations that are best preactivated for catalysis for β-D-glucopyranose are $^{2}S_{O}$ and $^{1}S_{3}$. It is remarkable that whereas the $^{1}S_{3}$ (and the neighbor $^{1,4}B$) is the preferred ring distorted conformation in Michaelis complexes of retaining β-glucosidases, the $^{2}S_{O}$ conformation seems to be the preferred conformation in inverting β-glucosidases, as discussed below. This indicates that glycosidases might have evolved to preferentially select those conformations of the substrate that both require less energy to be distorted and, at the same time, exhibit the highest oxocarbenium ion-like properties.

$^{4}C_{1} \leftrightarrow {}^{4}H_{3} \leftrightarrow {}^{1}S_{3}$ Retaining α-Glycosidases. It is likely that many retaining α-glycosidases will simply follow the reverse of the $^{1}S_{3} \rightarrow {}^{4}H_{3} \rightarrow {}^{4}C_{1}$ itinerary, described above, in which α-linked substrate binds in $^{4}C_{1}$ conformation (with the leaving group already correctly poised for in-line attack) and intermediate in $^{1}S_{3}$. This has been observed both for the GH31 α-glycosidases[24,25] and GH27 α-galactosidases.[26]

It is less clear what the itinerary of classical α-amylases and cyclodextrin glycosyltransferases, both from family GH13 and glucoamylases from GH15, adopt. From a structural perspective, the classical α-glucosidase inhibitor acarbose, whose inhibition constant is typically around the picomolar to nanomolar level, affords a facile route into obtaining complexes but its $^{2}H_{3}$ conformation cannot be interpreted as indicative of any likely reaction transition state. Kinetic isotope effect (KIE) work has suggested a $B_{2,5}$ transition state for a yeast α-glucosidase,[27] but beyond this there is little KIE insight for other systems. From a structural perspective, a key question had been the conformation adopted by the covalent intermediate of a retaining GH13 α-glucosidase but has been difficult to analyze structurally, perhaps hinting at their high reactivities. The first structure of a covalent intermediate, that of the cyclodextrin glucosyltransferase,[28] revealed the pyranosyl-enzyme in a $^{4}C_{1}$ chair conformation (thus with an equatorial linkage to the enzyme nucleophile; similar complexes have been observed on other related enzymes since) rather than one poised for facile nucleophilic attack in the second step of the retaining mechanism. While it seems reasonable that these transglycosidases use a more stable intermediate as a strategy to discourage hydrolysis of the intermediate (rather than transfer to a sugar acceptor), it is far less easy to interpret in light of the recent trapping of the intermediate on a hydrolytic α-amylase in the same $^{4}C_{1}$ chair conformation, albeit with an L-idosyl sugar.[29]

Itineraries around the $^{2,5}B$ Conformation ($^{2}S_{O}$, $^{2,5}B$): Inverting Glucosidases and Retaining Xylanases. Although the history of glycosidase work, with some notable exceptions, had largely considered half-chair transition states, it is now clear that all the possible pathways are utilized by specific enzymes. For example, the FEL of β-D glucose suggets $^{2}S_{O}$ as another conformation preactivated for catalysis,[22,23] and that is exactly what had previously been observed experimentally for a number of structurally distinct inverting β-glucosidases including GH6 inverting cellulases[30] (Figure 4a). $^{2}S_{O}$ most simply implies electrophilic migration through a $^{2,5}B$ conformation with support for this pathway coming from inhibitor distortion to this conformation[31] and modeling.[32] Strong support for this itinerary in inverting β-glucosidases comes from the observation of an $^{2}S_{O}/^{2,5}B$ conformed Michaelis complex of Cel8A (Figure 4a)[33] subsequently also analyzed by QM/MM metadynamics simulations.[34]

The $^{2,5}B$ conformation is not only the most likely TS structure in the above $^{2}S_{O} \rightarrow {}^{2,5}B$ itinerary for inverting β-glycosidases, but it has also been found to be the Michaelis structure or the covalent glycosyl−enzyme intermediate in some retaining GH families. In 1999, there were two reports of trapped glycosyl−enzyme intermediates of retaining GH11 xylanases in $^{2,5}B$ conformation.[35,36] Here there are additional caveats that prevent unambiguous interpretation; in most cases, structural complexes are observed which flank a potential transition state conformation. Here the intermediate itself is $^{2,5}B$, implying either a relaxation from the first formed intermediate or a transition state conformation poised close by. However, no Michaelis complexes for this enzyme class have yet been identified, although a recent modeling study on a GH11 retaining endo-β-1,4-xylanase from *B. circulans* concluded that the Michaelis complex is in $^{2,5}B$ conformation.[37]

Itineraries around $B_{2,5}$ ($^1S_5$, $B_{2,5}$, $^OS_2$): Retaining β- and (some) α-Mannosidases, and Some Inverting β-Mannosidases. One of the mysteries in the conformational analysis of glycosidases was how enzymes acting on α- or β-mannosides would achieve nucleophilic substitution at the anomeric center, given the severe *cis*-1,2 diaxial problems from the ground-state axial O2 that bedevil synthetic chemistry of mannosides. Furthermore, a "*gluco*−*manno* conundrum" was known to exist as many β-D-glucosidases were similar in sequence and structure to β-D-mannosidases and possessed the same recognition apparatus around the O2 position, despite the difference in configuration at C2 of their respective substrates. This posed intriguing questions about how specificity and catalysis were achieved.

Analysis of the Michaelis and trapped covalent intermediate complexes of the retaining *Cellvibrio japonicus* endo β-1,4-mannanase, Man26A,[38] provided the first insight into a new conformational itinerary. The Michaelis complex was observed in an $^1S_5$ conformation (Figure 4b) and the intermediate in $^OS_2$. Again, these conformations flank a potential transition state conformation, here $B_{2,5}$, having the beneficial coplanar arrangement of C2−C1−O5−C5, and again this seems the most likely itinerary for catalysis. This itinerary is consistent with electrophilic migration of C1 along the reaction coordinate and one that has been supported by subsequent mannanase Michaelis complexes in $^1S_5$ conformation including an unhydrolyzed mannooligosaccharide on a family GH26 mannobiohydrolase.[39] Furthermore, experimental data on the solution conformation of mannosyl moieties having "anomeric" sp^2 centers had, as far back as 1982, revealed a favored $B_{2,5}$ conformation for D-mannono-1,5-lactone prompting the authors to envisage boats in addition to half-chairs as TS structures.[40] A near $B_{2,5}$ transition state also avoids the *cis*-1,2 diaxial clashes during substitution events at the anomeric carbon and thus also resolves the gluco−manno conundrum, since both classes of enzyme recognize (pseudo)equatorial O2 substituents at the transition state. Persuasively, synthetic chemists have arrived at the same mechanistic conclusions with Crich's seminal use of 4,6-benzylidine acetal protection group chemistry also controlling mannosylations through manipulation of the O3−C3−C2−O2 torsional angle (reviewed in ref 41).

The proposals of a reaction coordinate passing through a $B_{2,5}$ conformation for mannoside hydrolysis has extensive support from diverse independent experiments and computational approaches, yet it has still aroused criticism from one group.[42] Therefore, in order to probe the transition state structure of β-mannosidases, a combined structural and linear-free energy relationship (LFER) approach was recently undertaken through the study of a panel of different mannosidase inhibitors.[43] These studies revealed that all tight-binding inhibitors are distorted to $B_{2,5}$ (for example, mannoimazazole, Figure 4b) or close conformations on-enzyme and that the free energy of binding of the inhibitor was correlated with the free energy of binding of the enzymatic transition state thus reinforcing the $B_{2,5}$ TS conformation. Another evidence of the $B_{2,5}$ transition state is provided by the computed conformational free energy landscape of β-mannose associated with the ideal Stoddart conformational diagram (Figure 4b),[23] which shows a clear low energy pathway in the $^1S_5 \leftrightarrow B_{2,5} \leftrightarrow {}^OS_2$ region. The most preactivated conformation in terms of energy, elongation/shortening of the C1−O1/C1−O5 bonds, C1−O1 orientation, and charge development at the anomeric carbon was found to be $^1S_5$, in agreement with the conformations observed crystallographically.

Such a pathway may not be solely limited to β-mannosidases. In 2003, covalent glycosyl enzyme intermediates of the retaining GH38 Golgi α-mannosidase II were trapped using two different compounds (5Fβ-L-GulF and 2Fα-D-ManF) and observed in the $^1S_5$ conformation. This conformation is exactly that previously observed for the β-linked Michaelis complex of retaining β-mannosidases,[38] leading Withers and colleagues to propose that catalysis would likely follow the reverse conformation pathway to retaining β-mannosidases (hence $^OS_2 \rightarrow B_{2,5} \rightarrow {}^1S_5$) passing through the $B_{2,5}$ at, or close to, the transition state. Likewise, more recent experimental[44] and QM/MM metadynamics[45] studies support a pathway for glycosylation that follows an $^OS_2/B_{2,5} \rightarrow [B_{2,5}]^{\ddagger} \rightarrow {}^1S_5$ itinerary.

Recently, the structure of a GH92 inverting α-mannosidases within diverse complexes was reported.[46] Although pathways here cannot be unambiguously described, as no competent Michaelis complexes are available, distortion of the mannoimidazole to approximately a $B_{2,5}$ conformation suggests a pathway around this conformation and would appear to rule out a "ring-flipped" pathway as adopted by GH47 inverting α-mannosidases, described below. Another mannosidase oddity is the GH125 inverting mannosidases which show no substrate distortion in their pseudo-Michaelis complex.[47] More analyses are clearly required to resolve these conundrums.

Southern Hemisphere Pathways around $^3H_4$: Some Inverting α-Mannosidases, and Retaining α-L-Fucosidases and Sialidases. Southern hemisphere and hence "ring-flipped" pathways are far rarer than their Northern hemisphere

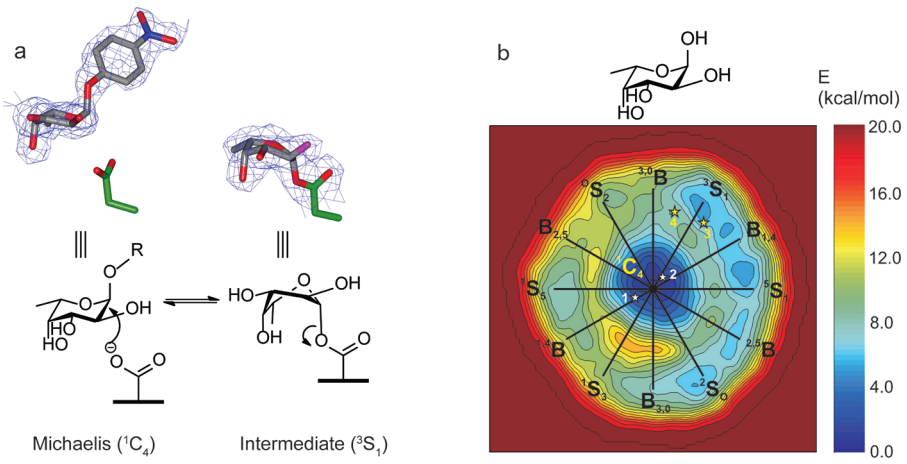

FIGURE 5. Conformational analysis of α-L-fucosidases. (a) Experimental electron densities for the trapping of the Michaelis[51] and intermediate[50,51] complexes of GH29 α-fucosidases exemplifying how analyses along a pathway can provide additional insight. (b) Computed FEL of α-L-fucose[51] with respect to ring distortion (Southern hemisphere of the Cremer–Pople sphere). Each contour line of the diagram corresponds to 0.5 kcal·mol^{-1}. Star symbols plot the observed conformations for a GH29 α-L-fucoside Michaelis complex (**1**) and an imino-sugar inhibitor (**2**). The two covalent intermediates are shown as **3**[51] and **4**.[50]

counterparts. This likely reflects the paucity of L-sugars in nature and also the large energy barriers associated with flipping a $^4C_1$ chair form for many (but not all) D-glycosides. One notable exception is the inverting GH47 α-mannosidases where structures in complex with both deoxymannojirimycin and kifunensine revealed a ring flipped $^1C_4$ conformation, mimicking either the Michaelis complex or the reaction product.[48] Again, consideration of these complexes in light of the pseudorotational itinerary strongly suggested catalysis through the adjacent $^3H_4$ transition state located in the Southern hemisphere of the conformational itinerary. Strong additional support for such an itinerary comes from the observation of a nonhydrolyzable thiodisaccharide substrate in which the −1 subsite is indeed distorted to a $^3S_1$ conformation consistent with a $^3S_1 \rightarrow {}^3H_4 \rightarrow {}^1C_4$ catalytic itinerary.[49]

L-Glycoside hydrolases have the option of a latitudinal pathway through a boat conformation or a longitudinal one via $^3H_4$. In 2004, Sulzenbacher and colleagues trapped the covalent intermediate of a retaining GH29 α-L-fucosidase,[50] observed in $^3S_1$ conformation. More recently, an intermediate ($^3S_1$) and Michaelis complex ($^1C_4$) of a *Bacteroides thetaiotaomicrometer* GH29 α-L-fucosidase[51] were also trapped (Figure 5). Together these analyses suggest that α-L-fucosides have a favored $^1C_4$ chair conformation for the substrate (in which the leaving group is axial and thus poised for in-line attack) with a $^1C_4 \rightarrow {}^3H_4 \rightarrow {}^3S_1$ pathway for the formation of the covalent intermediate. This is supported by ab initio metadynamics; the conformational FEL of α-L-fucose (Figure 5) reveals that the $^1C_4$ conformer is the most preactivated for catalysis.[51]

One group of glycosidases of major medical importance are the sialidases/neuraminidases. The first trapping of a retaining (trans)sialidase both in Michaelis complex and covalent intermediate[52] revealed a relaxed $^2C_5$ conformation for the intermediate (equating to $^1C_4$ for aldopyranosides considered elsewhere in this review), suggesting a conformational pathway for glycosylation that proceeds via a distorted substrate through $^4H_5 \rightarrow {}^2C_5$ equating to ($^3S_1 \rightarrow$) $^3H_4 \rightarrow {}^1C_4$ in the more classical aldopyranoside nomenclature. In this case, observation of the pyranose ring in different Michaelis complexes as a $^6S_2$ and $B_{2,5}$ (equating to $^5S_1/B_{1,4}$) is not unambiguously supportive of any one pathway, as these are also close to other possible conformational routes. More recently, there have been reported trappings of a number of covalent tyrosyl–enzyme intermediates for sialidases, all showing $^2C_5$ conformations for the intermediate. All of these, however, suggest catalysis proceeds through a transition state close to $^4H_5$ conformation (which is indeed adopted by the anti-influenza drug oseltamivir).

Distortion and Beyond

A major direction for the field is to use conformational insight to generate specific enzyme inhibitors; as both cellular probes and therapeutic agents. Generic inhibitors, such as aza and imino sugars are very powerful, but they generally lack specificity. So while the destination of specific conformational mimicry remains, routes to it are less clear. Initial crude attempts simply to append bridging functions fail because the appended functions simply clash

with the enzyme surface.[43] There are few examples of conformationally specific inhibitors; one example is the kifunensines whose $^{1}C_{4}$ conformation renders them very good inhibitors of GH47 mannosidases (reflecting their $^{3}S_{1} \rightarrow {}^{3}H_{4} \rightarrow {}^{1}C_{4}$ catalytic itinerary)[48] but far poorer inhibitors of GH38 mannosidases (that likely use a near-$B_{2,5}$ transition state). It is clear that there is scope for inspired solutions to these problems based upon the conformational analyses, but such solutions have yet to be found. Recent work by Schramm,[53] Vocadlo,[54] and their colleagues points the way forward: rigorous analysis of reaction mechanism and transition state poise, followed by design and in vivo application of specific mechanism-based inhibitors.

It is now clear that structural insight shows stable species that flank or neighbor all four of the transition state conformations and that different enzymes utilize different pathways. While structural biology can provide insight into conformational pathways, it can provide neither transition state poise nor the dynamics; these will always remain the domain of experimental physical-organic chemistry or, increasingly, computation. One can make reasonable predictions as to reaction coordinate. Mannosidases likely use itineraries centered around the $^{3}H_{4}$ or $B_{2,5}$ conformations, that place O2 pseudoequatorial, a facet that has allowed specific inhibition reflecting the different transition state structures. Most retaining enzymes acting on β-D-*gluco*-configured substrates use $^{4}H_{3}$ centered pathways, and all inverting enzymes of this type, studied thus far, and perhaps family GH11 retaining xylanases, likely use $^{2,5}B$ dominated routes. The "ring-flipped" L-sugars, not surprisingly, lie in the "Southern hemisphere" $^{3}H_{4}$ region of the pseudorotational itinerary. Retaining and inverting α-D-glucosidases still remain a confusing area; clearly some of these enzymes operate via $^{4}C_{1} \leftrightarrow {}^{4}H_{3} \leftrightarrow {}^{1}S_{3}$ pathways, as predicted from the reverse of α-D-glucosidase pathways, but for many enzymes it is simply not known what pathway and transition state they favor.

The analysis of conformational preference is clearly an area of study where computational work is having an increasing impact. Recent work in mapping the conformational free energy landscape of pyranoses has revealed that the factors governing the distortion of the -1 sugar unit in GHs are largely dictated by the intrinsic properties of the free sugar unit and that enzyme–substrate interactions may have evolved to fulfill all of the criteria required for efficient catalysis. Moreover, inspection of the free energy landscapes highlights potential conformational itineraries in glycosidase catalysis which conform to those that are being both observed and computed for enzymatic reactions.

G.J.D. is a Royal-Society/Wolfson Research Merit Award recipient with current funding from the BBSRC and the EPSRC. C.R. and A.P. acknowledge the financial assistance from GENCAT (2009SGR-1309 and 2009SGR-82) and MICINN (FIS2008-03845 and BFU2010-22209-C02-02).

Note Added after ASAP Publication. This paper was posted to the web on September 16, 2011 with an error in Figure 3. The corrected version was published on September 21, 2011.

BIOGRAPHICAL INFORMATION

Gideon J. Davies studied for his Ph.D. in Bristol before moving via EMBL Hamburg to the University of York where he is Professor of Chemistry. His area of expertise is the structural and mechanstic basis of catalysis in the area of carbohydrate-active enzymes.

Antoni Planas is Professor of Biochemistry and Head of the Bioengineering Department at the Institut Químic de Sarrià (IQS), Universitat Ramon Llull in Barcelona. He obtained his Ph.D. in Organic Chemistry by IQS, conducted postdoctoral research at UC Berkeley (with Prof. Jack Kirsch), and was Research Associate at the Autonomus University of Barcelona. He established his research group at the IQS in 1993. Research interests are on structure/function and protein engineering of carbohydrate-active enzymes.

Carme Rovira is ICREA Research Professor at Parc Científic de Barcelona (PCB). She obtained her Ph.D. in Chemistry from the University of Barcelona in 1995 and conducted postdoctoral research at the Max-Planck-Institut für Festkörperforschung (with M. Parrinello). Research interests are on the description of electronic processes in proteins by means of ab initio molecular dynamics.

FOOTNOTES

*To whom correspondence should be addressed. E-mail: davies@ysbl.york.ac.uk (G.J.D.); crovira@pcb.ub.es (C.R.).

REFERENCES

1 Cantarel, B. L.; Coutinho, P. M.; Rancurel, C.; Bernard, T.; Lombard, V.; Henrissat, B. The Carbohydrate-Active EnZymes database (CAZy): an expert resource for Glycogenomics. *Nucleic Acids Res.* **2009**, *37*, D233–D238.

2 Koshland, D. E. Stereochemistry and the mechanism of enzymatic reactions. *Biol. Rev.* **1953**, *28*, 416–436.

3 Sinnott, M. L. Catalytic mechanisms of enzymic glycosyl transfer. *Chem. Rev.* **1990**, *90*, 1171–1202.

4 IUPAC-IUB Joint Commission on Biochemical Nomenclature (JCBN).. Conformational nomenclature for five and six-membered ring forms of monosaccharides and their derivatives. *Eur. J. Biochem.* **1980**, *111*, 295–298.

5 Stoddart, J. F. *Stereochemistry of Carbohydrates*; Wiley Interscience: Toronto, 1971.

6 Phillips, D. C. Hen Egg-White Lysozyme molecule. *Proc. Natl. Acad. Sci. U.S.A.* **1967**, *57*, 484–495.

7 Vocadlo, D. J.; Davies, G. J.; Laine, R.; Withers, S. G. Catalysis by hen egg-white lysozyme proceeds via a covalent intermediate. *Nature* **2001**, *412*, 835–838.

8 Pauling, L. Molecular architecture and biological reactions. *Chem. Eng. News* **1946**, *24*, 1375–1377.

9 Ford, L. O.; Johnson, L. N.; Machin, P. A.; Phillips, D. C.; Tijan, T. Crystal structure of a lysozyme-tetrasaccharide lactone complex. *J. Mol. Biol.* **1974**, *88*, 349–371.

10 Tews, I.; Perrakis, A.; Oppenheim, A.; Dauter, Z.; Wilson, K. S.; Vorgias, C. E. Bacterial chitobiase structure provides insight into catalytic mechanism and the basis of Tay-Sachs disease. *Nat. Struct. Biol.* **1996**, *3*, 638–648.

11 Sulzenbacher, G.; Driguez, H.; Henrissat, B.; Schülein, M.; Davies, G. J. Structure of the Fusarium oxysporum endoglucanase I with a non-hydrolysable substrate analogue: substrate distortion gives rise to a pseudo-axial orientation for the leaving group. *Biochemistry* **1996**, *35*, 15280–15287.

12 Davies, G. J.; Wilson, K. S.; Henrissat, B. Nomenclature for sugar-binding subsites in glycosyl hydrolases. *Biochem. J.* **1997**, *321*, 557–559.

13 Davies, G. J.; Mackenzie, L.; Varrot, A.; Dauter, M.; Brzozowski, A. M.; Schülein, M.; Withers, S. G. Snapshots along an enzymatic reaction coordinate: analysis of a retaining β-glycoside hydrolase. *Biochemistry* **1998**, *37*, 11707–11713.

14 van Aalten, D. M. F.; Komander, D.; Synstad, B.; Gaseidnes, S.; Peter, M. G.; Eijsink, V. G. H. Structural insights into the catalytic mechanism of a family 18 exo-Chitinase. *Proc. Natl. Acad. Sci. U.S.A.* **2001**, *98*, 8979–8984.

15 Money, V. A.; Smith, N. L.; Scaffidi, A.; Stick, R. V.; Gilbert, H. J.; Davies, G. J. Substrate distortion by a lichenase highlights the different conformational itineraries harnessed by related glycoside hydrolases. *Angew. Chem., Int. Ed.* **2006**, *45*, 5136–5140.

16 Czjzek, M.; Ben David, A.; Braman, T.; Shoham, G.; Henrissat, B.; Shoham, Y. Enzyme-substrate complex structures of a GH39 beta-xylosidase from Geobacillus stearothermophilus. *J. Biol. Chem.* **2005**, *353*, 838–846.

17 He, Y.; Macauley, M. S.; Stubbs, K. A.; Vocadlo, D. J.; Davies, G. J. Visualizing the reaction coordinate of an O-GlcNAc hydrolase. *J. Am. Chem. Soc.* **2010**, *132*, 1807–1809.

18 Biarnes, X.; Nieto, J.; Planas, A.; Rovira, C. Substrate distortion in the michaelis complex of Bacillus 1,3-1,4-beta-glucanase - Insight from first principles molecular dynamics simulations. *J. Biol. Chem.* **2006**, *281*, 1432–1441.

19 Laio, A.; Parrinello, M. Escaping free-energy minima. *Proc. Natl. Acad. Sci. U.S.A.* **2002**, *99*, 12562–12566.

20 Cremer, D.; Pople, J. A. General definition of ring puckering coordinates. *J. Am. Chem. Soc.* **1975**, *97*, 1354–1358.

21 Spiwok, V.; Kralova, B.; Tvaroska, I. Modelling of beta-D-glucopyranose ring distortion in different force fields: a metadynamics study. *Carbohydr. Res.* **2010**, *345*, 530–7.

22 Biarnes, X.; Ardevol, A.; Planas, A.; Rovira, C.; Laio, A.; Parrinello, M. The conformational free energy landscape of beta-D-glucopyranose. Implications for substrate preactivation in beta-glucoside hydrolases. *J. Am. Chem. Soc.* **2007**, *129*, 10686–10693.

23 Ardevol, A.; Biarnes, X.; Planas, A.; Rovira, C. The conformational free-energy landscape of beta-D-mannopyranose: evidence for a $^{1}S_{5} \rightarrow B_{2,5} \rightarrow {}^{O}S_{2}$ catalytic itinerary in beta-mannosidases. *J. Am. Chem. Soc.* **2010**, *132*, 16058–16065.

24 Lovering, A. L.; Lee, S. S.; Kim, Y. W.; Withers, S. G.; Strynadka, N. C. J. Mechanistic and structural analysis of a family 31 alpha-glycosidase and its glycosyl-enzyme intermediate. *J. Biol. Chem.* **2005**, *280*, 2105–2115.

25 Kim, Y. W.; Lovering, A. L.; Chen, H. M.; Kantner, T.; McIntosh, L. P.; Strynadka, N. C. J.; Withers, S. G. Expanding the thioglycoligase strategy to the synthesis of alpha-linked thioglycosides allows structural investigation of the parent enzyme/substrate complex. *J. Am. Chem. Soc.* **2006**, *128*, 2202–2203.

26 Guce, A. I.; Clark, N. E.; Salgado, E. N.; Ivanen, D. R.; Kulminskaya, A. A.; Brumer, H.; Garman, S. C. Catalytic Mechanism of Human alpha-Galactosidase. *J. Biol. Chem.* **2010**, *285*, 3625–3632.

27 Hosie, L.; Sinnott, M. L. Effects of deuterium substitution alpha and beta to the reaction center, O-18 substitution in the leaving group, and aglycone acidity on hydrolyses of aryl glucosides and glucosyl pyridinium ions by yeast alpha-glucosidase - a probable failure of the antiperiplanar-lone-pair hypothesis in glycosidase catalysis. *Biochem. J.* **1985**, *226*, 437–446.

28 Uitdehaag, J. C. M.; Mosi, R.; Kalk, K. H.; B A, v. d. V.; Dijkhuizen, L.; Withers, S. G.; Dijkstra, B. W. Catalysis in the α-amylase family - X-ray structures along the reaction pathway of cyclodextrin glycosyltransferase. *Nat. Struct. Biol.* **1999**, *6*, 432–436.

29 Zhang, R.; Li, C.; Williams, L. K.; Rempel, B. P.; Brayer, G. D.; Withers, S. G. Directed "in Situ" Inhibitor Elongation as a Strategy To Structurally Characterize the Covalent Glycosyl-Enzyme Intermediate of Human Pancreatic alpha-Amylase. *Biochemistry* **2009**, *48*, 10752–10764.

30 Zou, J.-Y.; Kleywegt, G. J.; Stahlberg, J.; Driguez, H.; Nerinckx, W.; Claeyssens, M.; Koivula, A.; Teeri, T. T.; Jones, T. A. Crystallographic evidence for substrate ring distortion and protein conformational changes during catalysis in cellobiohydrolase Cel6A from Trichoderma reesei. *Structure* **1999**, *7*, 1035–1045.

31 Varrot, A.; Leydier, S.; Pell, G.; Macdonald, J. M.; Stick, R. V.; Gilbert, H. J.; Davies, G. J. Mycobacterium tuberculosis strains possess functional cellulases. *J. Biol. Chem.* **2005**, *280*, 20181–20184.

32 Koivula, A.; Ruohonen, L.; Wohlfahrt, G.; Reinikainen, T.; Teeri, T. T.; Piens, K.; Claeyssens, M.; Weber, M.; Vasella, A.; Becker, D.; Sinnott, M. L.; Zou, J. Y.; Kleywegt, G. J.; Szardenings, M.; Stahlberg, J.; Jones, T. A. The active site of cellobiohydrolase Cel6A from Trichoderma reesei: The roles of aspartic acids D221 and D175. *J. Am. Chem. Soc.* **2002**, *124*, 10015–10024.

33 Guerin, D. M. A.; Lascombe, M. B.; Costabel, M.; Souchon, H.; Lamzin, V.; Beguin, P.; Alzari, P. M. Atomic (0.94 angstrom) resolution structure of an inverting glycosidase in complex with substrate. *J. Biol. Chem.* **2002**, *316*, 1061–1069.

34 Petersen, L.; Ardevol, A.; Rovira, C.; Reilly, P. J. Mechanism of cellulose hydrolysis by inverting GH8 endoglucanases: a QM/MM metadynamics study. *J. Phys. Chem. B* **2009**, *113*, 7331–7339.

35 Sidhu, G.; Withers, S. G.; Nguyen, N. T.; McIntosh, L. P.; Ziser, L.; Brayer, G. D. Sugar ring distortion in the glycosyl-enzyme intermediate of a family G/11 xylanase. *Biochemistry* **1999**, *38*, 5346–5354.

36 Sabini, E.; Sulzenbacher, G.; Dauter, M.; Dauter, Z.; Jørgensen, P. L.; Schülein, M.; Dupont, C.; Davies, G. J.; Wilson, K. S. Structure of the Bacillus agaradhaerens family 11 xylanase and its catalytic intermediate: ^{2,5}B conformation for the glycosyl-enzyme intermediate and substrate specificity in glycoside hydrolase clan GH-C. *Chem. Biol.* **1999**, *6*, 483–492.

37 Soliman, M. E.; Ruggiero, G. D.; Pernia, J. J.; Greig, I. R.; Williams, I. H. Computational mutagenesis reveals the role of active-site tyrosine in stabilising a boat conformation for the substrate: QM/MM molecular dynamics studies of wild-type and mutant xylanases. *Org. Biomol. Chem.* **2009**, *7*, 460–468.

38 Ducros, V.; Zechel, D. L.; Murshudov, G. N.; Gilbert, H. J.; Szabo, L.; Stoll, D.; Withers, S. G.; Davies, G. J. Substrate distortion by a β-mannanase: Snapshots of the Michaelis and covalent intermediate complexes suggest a $B_{2,5}$ conformation for the transition-state. *Angew. Chem., Int. Ed.* **2002**, *41*, 2824–2827.

39 Cartmell, A.; Topakas, E.; Ducros, V. M.-A.; Suits, M. D.; Davies, G. J.; Gilbert, H. J. The Cellvibrio japonicus mannanase CjMan26c displays a unique exo-mode of action that is conferred by subtle changes to the distal region of the active site. *J. Biol. Chem.* **2008**, *283*, 34403–34413.

40 Walaszek, Z.; Horton, D.; Ekiel, I. Conformational studies on aldonolactones by NMR spectroscopy. Conformations of D-glucono-1,5-lactone and D-manno-1,5-lactone in solution. *Carbohydr. Res.* **1982**, *106*, 193–201.

41 Crich, D. Mechanism of a Chemical Glycosylation Reaction. *Acc. Chem. Res.* **2010**, *43*, 1144–1153.

42 Nerinckx, W.; Daesmet, T.; Claeyssens, M. Itineraries of enzymatically and non-enzymatically catalyzed substitutions at *O*-glycopyranosidic bonds. *ARKIVOC* **2006**, *13*, 90–116.

43 Tailford, L. N.; Offen, W. A.; Smith, N. L.; Dumon, C.; Morland, C.; Gratien, J.; Heck, M.-P.; Stick, R. V.; Blériot, Y.; Vasella, A.; Gilbert, H. J.; Davies, G. J. Structural and biochemical evidence for a boat-like transition state in β-mannosidases. *Nat. Chem. Biol.* **2008**, *4*, 306–312.

44 Zhong, W.; Kuntz, D. A.; Ember, B.; Singh, H.; Moremen, K. W.; Rose, D. R.; Boons, G. J. Probing the substrate specificity of Golgi alpha-mannosidase II by use of synthetic oligosaccharides and a catalytic nucleophile mutant. *J. Am. Chem. Soc.* **2008**, *130*, 8975–8983.

45 Petersen, L.; Ardevol, A.; Rovira, C.; Reilly, P. J. Molecular mechanism of the glycosylation step catalyzed by Golgi alpha-mannosidase II: a QM/MM metadynamics investigation. *J. Am. Chem. Soc.* **2010**, *132*, 8291–8300.

46 Zhu, Y.; Suits, M. D.; Thompson, A. J.; Chavan, S.; Dinev, Z.; Dumon, C.; Smith, N.; Moremen, K.; Xiang, Y.; Siriwardena, A.; Williams, S. J.; Gilbert, H. J.; Davies, G. J. Mechanistic insights into a calcium-dependent family of α-mannosidases in a human gut symbiont. *Nat. Chem. Biol.* **2010**, *6*, 125–132.

47 Gregg, K. J.; Zandberg, W. F.; Hehemann, J. H.; Whitworth, G. E.; Deng, L. H.; Vocadlo, D. J.; Boraston, A. B. Analysis of a New Family of Widely Distributed Metal-independent alpha-Mannosidases Provides Unique Insight into the Processing of N-Linked Glycans. *J. Biol. Chem.* **2011**, *286*, 15586–15596.

48 Vallee, F.; Karaveg, K.; Herscovics, A.; Moremen, K. W.; Howell, P. L. Structural basis for catalysis and inhibition of N-glycan processing class I alpha 1,2-mannosidases. *J. Biol. Chem.* **2000**, *275*, 41287–41298.

49 Karaveg, K.; Siriwardena, A.; Tempel, W.; Liu, Z. J.; Glushka, J.; Wang, B. C.; Moremen, K. W. Mechanism of class 1 (Glycosylhydrolase family 47) alpha-mannosidases involved in N-glycan processing and endoplasmic reticulum quality control. *J. Biol. Chem.* **2005**, *280*, 16197–16207.

50 Sulzenbacher, G.; Bignon, C.; Nishimura, T.; Tarling, C. A.; Withers, S. G.; Henrissat, B.; Bourne, Y. Crystal structure of Thermotoga maritima alpha-L-fucosidase - Insights into the catalytic mechanism and the molecular basis for fucosidosis. *J. Biol. Chem.* **2004**, *279*, 13119–13128.

51 Lammerts van Bueren, A.; Ardèvol, A.; Fayers-Kerr, J.; Luo, B.; Zhang, Y.; Sollogoub, M.; Blériot, Y.; Rovira, C.; Davies, G. J. Analysis of the reaction coordinate of α-L fucosidases: a combined structural and quantum mechanical approach. *J. Am. Chem. Soc.* **2010**, *132*, 1804–1806.

52 Amaya, M. F.; Watts, A. G.; Damager, T.; Wehenkel, A.; Nguyen, T.; Buschiazzo, A.; Paris, G.; Frasch, A. C.; Withers, S. G.; Alzari, P. M. Structural insights into the catalytic mechanism of Trypanosoma cruzi trans-sialidase. *Structure* **2004**, *12*, 775–784.

53 Kicska, G. A.; Long, L.; Horig, H.; Fairchild, C.; Tyler, P. C.; Furneaux, R. H.; Schramm, V. L.; Kaufman, H. L. Immucillin H, a powerful transition-state analog inhibitor of purine nucleoside phosphorylase, selectively inhibits human T lymphocytes. *Proc. Natl. Acad. Sci. U.S.A.* **2001**, *98*, 4593–4598.

54 Yuzwa, S. A.; Macauley, M. S.; Heinonen, J. E.; Shan, X.; Dennis, R. J.; He, Y.; Whitworth, G. E.; Stubbs, K. A.; McEachern, E. J.; Davies, G. J.; Vocadlo, D. J. A potent mechanism-inspired O-GlcNAcase inhibitor that blocks phosphorylation of tau in vivo. *Nat. Chem. Biol.* **2008**, *4*, 483–490.